

Turbulence Transition and Its Role in Isotope Effects of LHD

Kinoshita, T.
RIAM, Kyushu university

Tanaka, K.
National Institute for Fusion Science

Ishizawa, A.
Graduate School of Energy Science, Kyoto University

Nunami, M.
National Institute for Fusion Science

他

<https://hdl.handle.net/2324/7183316>

出版情報 : 2023-10. International Atomic Energy Agency
バージョン :
権利関係 :

TURBULENCE TRANSITION AND ITS ROLE IN ISOTOPE EFFECTS OF LHD

T. Kinoshita

RIAM, Kyushu university

Kasuga, Japan

Email: t.kinoshita@triam.kyushu-u.ac.jp

K. Tanaka

National Institute for Fusion Science

Toki, Japan

IGSES, Kyushu university

Kasuga, Japan

A. Ishizawa

Graduate School of Energy Science, Kyoto University

Uji, Japan

M. Nunami

National Institute for Fusion Science

Toki, Japan

Graduate School of Energy Science, Kyoto University

Uji, Japan

H. Sakai

IGSES, Kyushu university

Kasuga, Japan

Abstract

In this study, we discover a turbulence transition and its role in the isotope effects in the Large Helical Device (LHD). The turbulence levels and turbulence-driven transports decrease with an increase in the electron density to a specific density; however, they increase in regimes above the density. Density scan experiments and gyrokinetic/MHD simulations reveal that the observed ion-scale turbulence is the ion-temperature gradient (ITG) turbulence below the density and resistive-interchange (RI) above the density. Negligible isotope effects in the turbulences and transports of hydrogen (H) and deuterium (D) plasma were found in the ITG regime. However, clear isotope effects were observed in the RI regime. In the RI regime, the turbulences and transports were clearly suppressed, and the confinements were improved in D plasma. The reduction of the turbulence level in the RI regime of the D plasma is likely due to the heavier ion mass and lower resistivity in D plasma, which suppress the linear growth rate of RI turbulence.

1. INTRODUCTION

Isotope effect studies of plasma confinement with hydrogen and deuterium are imperative for the performance prediction of a fusion power plant with deuterium and tritium. Transport in plasmas cannot be accounted for only by neoclassical transport, and turbulence-driven transport plays an significant role in confinement degradation. Transport in tokamaks shows a different ion mass dependence from gyro-Bohm prediction, but has recently been found to be explained by several turbulence suppression mechanisms in heavier ion-mass plasmas [1]. Stellarators/heliotrons are an alternative concept, which have the advantages of being current-disruption free and not requiring a plasma-current drive. Deuterium experiments in the stellarator/heliotron device had been conducted in ATF, CHS, Heliotron-E, and W7-AS before 2017, but compared to the tokamaks, knowledge was scarce and no clear isotope effects in confinement were observed [2–5]. However, with the beginning of deuterium experiments at LHD in 2017, systematic studies in ECRH plasma provided improved deuterium plasma confinement similar to the tokamaks [6–9]. It has been reported that the isotope effect of neoclassical transport is small in LHD, and most of the appearance of the isotope effect in confinement can be attributed to the isotope effect of anomalous transport driven by turbulence. Particularly, in the electron cyclotron resonance heating (ECRH) plasma, in which the ion mass dependence is pronounced, the contribution of fast ions due to neutral beam injection can be eliminated in addition to the electric field shear (at balanced injection) and impurities (without impurity puffing) that contribute to the stabilization of turbulence in the tokamaks. This result implies the existence of a physical mechanism for confinement improvement that is different from that of tokamaks, and the elucidation of this mechanism is essential for predicting the performance of a stellarator/heliotron D-T

fusion reactor. This study focuses on this point and aims to understand the physical mechanism of confinement improvement at LHD through turbulence measurements and its role in energy and particle transports.

2. EXPERIMENTAL SETUP

In this study, we shed light on ECRH plasmas. This is because in addition to the clear isotope effects observed in ECRH plasmas in previous studies [9], and external turbulent stabilization, such as fast ion and electric field shear associated with neutral beam injection reported in tokamaks can be neglected [10, 11]. To clarify the isotope effects of turbulence and transport, systematic density-scan experiments were performed in which only ion species were replaced by hydrogen (H) and deuterium (D) under constant heating conditions. The magnetic configuration is the magnetic axis position $R_{ax} = 3.6$ m and toroidal field strength $B_t = 2.75$ T, which is the best confinement performance in the International Stellarator Scaling 2004 (ISS04) [5] data set. Two 154 GHz microwave second harmonic micro waves was injected tangentially co and counter to B_t simultaneously to cancel out EC-driven current. Ion-scale electron density fluctuations with the poloidal wavenumber $k=0.1-0.8\text{mm}^{-1}$ were measured in the frequency range $f=32-500$ kHz using two-dimensional phase contrast imaging (2D-PCI) [12, 13]. Simultaneously, the electron density was modulated at 1.25 Hz by H2 or D2 gas puffing to evaluate the particle transport.

3. CONFINEMENT TIME

First, the dependence of the global energy confinement time $\tau_{E\text{ kin}}$ on the line-averaged electron density \bar{n}_e in the H and D plasmas are shown in Figure 1. In the H plasma, $\tau_{E\text{ kin}}$ increases linearly with increasing \bar{n}_e and moderates above $\bar{n}_e = 1.5 \times 10^{19}\text{m}^{-3}$, indicated by the dashed blue line. In the D plasma, a similar change in dependence appears at $\bar{n}_e = 2.5 \times 10^{19}\text{m}^{-3}$ indicated by the red dashed line. In this article, the density regime below the dashed line is called the "low-density regime" and the region above the dashed line is the "high-density regime". Focusing on the isotope effect, no clear isotope effect appears in the low-density regime, whereas the confinement is significantly improved in D plasmas at the high-density regime. This is important evidence for the appearance of isotope effects in LHD, which has already been reported in previous studies [8]. However, the favorable confinement in the D plasma cannot be accounted for by the improved mechanism in tokamaks and has not yet been resolved.

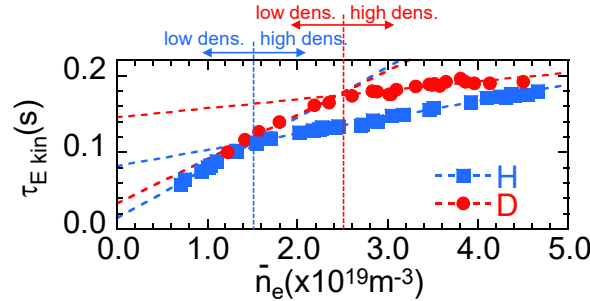


FIG. 1. Electron-density dependence of global energy confinement time

4. TYPICAL PROFILES IN LOW- AND HIGH-DENSITY REGIME

The temperature and density profiles are the result of energy and particle transport and are suitable for confirming the existence of isotope effects. The electron and ion temperature profiles have a similar shape in the low-density regime as shown in Fig. 2(a-1), whereas the higher electron density are observed in the D plasma in the high-density regime as shown in Fig. 2(b-1). The achievement of higher electron temperatures in the D plasma is partly attributed to the increased ion heating power because of the equal-dispersion law of energy, but also the reduced turbulence-driven electron energy transport noted in previous studies [7]. Similarly, the electron density has a similar profile shape in the H and D plasmas at the low-density regime as shown in Figure 2(a-2) however in the high-density regime, the D plasma has a more hollow profile than the H plasma as shown in Figure 2(b-2). There are several possibilities for the formation of different electron density profiles, for example, the penetration length of gas puffs, impurity profiles, and the contribution of particle transport. The right-hand scale of Fig. 2(a-2) and (b-2) shows the particle source profile calculated by three-dimensional neutral particle transport simulation code EIRENE [14]. Owing to the larger ion mass of deuterium, the particle source penetration depth is slightly shallower in

the D plasma than in the H plasma, but this slight difference does not account for the difference in the electron density profile. The main impurity in LHD is carbon ions (C^{6+}) produced by physical and chemical sputtering of carbon divertor plates. Figs. 2(a-3) and (b-3) show the carbon ion density profiles measured by the charge exchange recombination spectroscopy(CXRS). Regardless of density, the amount of carbon is approximately four times greater in the D plasma. This is due to the greater sputtering in the high-mass D plasma [15]. The profile shape of carbon is hollow in the low-density regime and peaked in the high-density regime, suggesting that the impurity transport is also different in the density regime. However, the contribution of carbon to the electron density is 1.5% and 7% in H and D plasmas, respectively, and cannot account for the hollow electron density distribution in D plasma. Therefore, the difference of the electron density profile shown in 2(b-2) can be attributed to the contribution of particle transport. At the same time, from Figs. 2(a-4) and (b-4), the turbulence level \tilde{n}_e/n_e normalized by the electron density shows isotope effects only in the high-density regime, which is consistent with improved confinement in D plasmas. As described above, the profile comparison typical H and D plasmas suggests the existence of isotope effects in turbulence-driven energy and particle transport in the high-density regime.

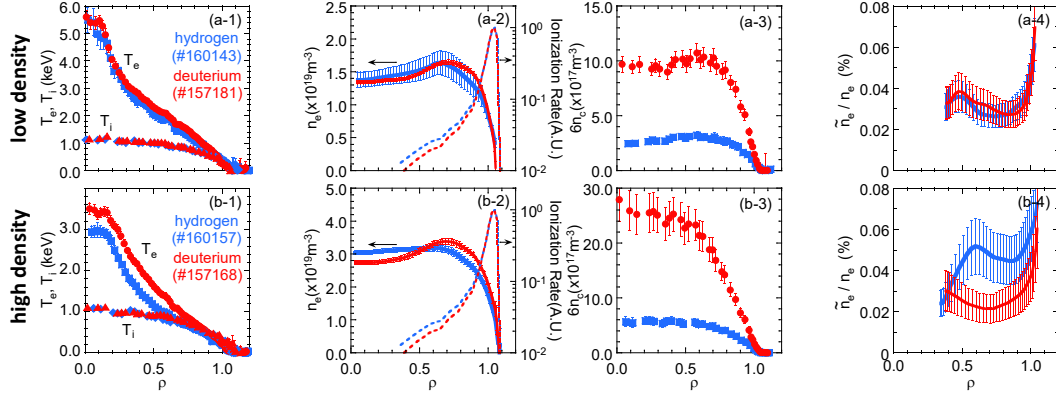


FIG. 2. Comparison of H and D plasma distribution in low and high density regime. (a-) low-density region (H: #160143 D: #157181), (b-) high-density region (H: #160157, D: #157168), (-1) electron and ion temperatures (-2) electron density and particle source shape, (-3) carbon density and (-4) turbulence level(\tilde{n}_e/n_e). Here, ρ is a normalized radius which is defined as r_{eff}/a_{99} . r_{eff} is an averaged minor radius and a_{99} is the averaged minor radius where 99% of kinetic energy is confined inside. Here, the electron number 6 is multiplied to visualize the effect of carbon on the electron density.

5. RELATION BETWEEN TURBULENCE AND TRANSPORT

5.1. Ion-scale turbulence

As noted above, isotope effects are found in the high-density regime, suggesting that improved confinement and higher temperatures in D plasmas are associated with turbulence suppression in D plasmas. To clarify these relationship in detail, the density dependence of the turbulence level \tilde{n}_e/n_e and its phase velocity in the plasma flame V_{turb} are demonstrated in Figures 3 (a) and (b), respectively. Here, the average value at the normalized radius $\rho=0.5-0.7$ was used, where the turbulence behavior changed significantly in a series of experiments. As shown in Fig. 3(a), in both H and D plasmas, the turbulence level first decreases with an increase in the electron density and after reaching a minimum value, it rises again. Moreover, the turbulence levels are comparable in the low-density H and D plasmas; however the level is clearly lower in the high-density D plasma. In a previous study [11], gyrokinetic simulations with fixed temperature density profiles and $E \times B$ shear and different ion species showed that the linear growth rate of the ion temperature gradient (ITG) turbulence is suppressed in plasmas with heavy ion masses. However, as shown in Fig. 3(b), the turbulence propagates in the ion-diamagnetic direction in the low-density regime, whereas the high-density regime is in the electron-diamagnetic direction and strongly suggests that the measured turbulence is not ITG and that it has transited to another mode of turbulence.

5.2. Energy and particle transport

Figures 4(a) and (b) are the electron density dependence of the anomalous contribution of electron energy transport $\chi_{e\,ano}$ and ion energy transport $\chi_{i\,ano}$ averaged at $\rho=0.5-0.7$. The anomalous contributions are defined as subtracting the neoclassical value from the experimental value. The experimental values were evaluated from a power-balance analysis using LHDGAUSS [16] and TASK3D [17], and the neoclassical values were calculated using GSRAKE [18]. In the low-density

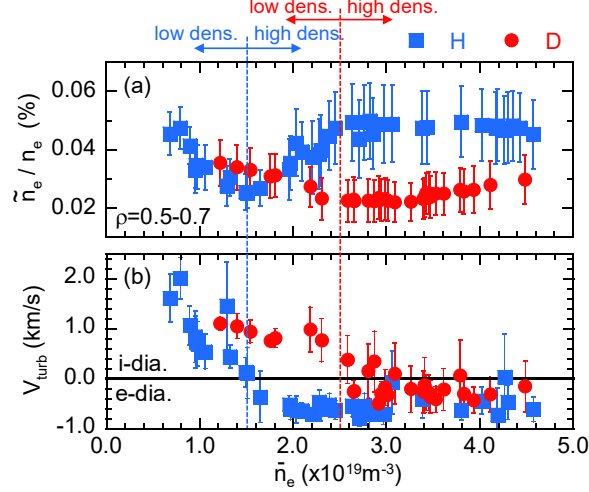


FIG. 3. Electron-density dependence of the (a) ion-scale turbulence level and (b) its phase velocity in the plasma frame. The blue and red symbols indicate H plasma and D plasma, respectively.

regime, $\chi_{e\text{ ano}}$ decreases with increasing electron density and no clear isotope effects are observed. In contrast, in the high-density regime, $\chi_{e\text{ ano}}$ increases with increasing electron density and is suppressed in D plasmas. On the other hand, although $\chi_{i\text{ ano}}$ is almost zero or negative in low-density regions, in high-density regions, $\chi_{i\text{ ano}}$ behaves similarly to $\chi_{e\text{ ano}}$. The density dependence and isotope effects are identical to the trends observed in the ion-scale turbulence except for $\chi_{i\text{ ano}}$ in the low-density regime, suggesting that the measured ion-scale turbulence play a significant role in the energy transport.

In practice, the electron density fluctuations contribute mainly to particle flux; therefore, the isotope effects in particle transport should be discussed as well [19]. However, compared with energy transport [1, 5, 8, 20–23], the knowledge of isotope effects on particle transport are limited [7, 9, 24]. The reason for this is the difficulty of the estimation of the particle transport coefficients owing to the two physics characteristics. The former is the estimation of particle fueling due to the ionization of fueling gas. The second characteristic is the existence of the off diagonal terms. In this study, density modulation experiments were performed to evaluate particle transport. The density modulation technique is originally proposed by K. W. Gentle [25] and has already been conducted in LHD [7, 26–28]. The advantages of the density modulation experiment are that the diffusion coefficient ($D_{e\text{ mod}}$) and convection velocity ($V_{e\text{ mod}}$) are evaluated simultaneously, and absolute values of the particle fuels are not required. In this study, the model fitting of the diffusion coefficient ($D_{e\text{ mod}}$) and convection velocity ($V_{e\text{ mod}}$) were using Generic Algorithm and Quasi-Newton method [26] and the radial profiles of the particle sources calculated by the 3D neutral particle transport simulation code EIRENE [14] were used as shown in Figs. 2(a-1) and (b-1).

Figures 4(c) and (d) show the electron density dependence of the anomalous contributions of the diffusion coefficient $D_{e\text{ ano}}$ and the convection velocity $V_{e\text{ ano}}$ at $\rho=0.7-0.9$. The reason why $\rho=0.5-0.7$ is not shown here is that the modulation component due to gas puffing with 1.25 Hz did not propagate to $\rho < 0.7$ in the high-density regime owing to a good confinement. In the low-density regime, the adjustment of the gas supply for density modulation in the D plasma did not work well, and the density modulation experiment could not be performed. As shown in Figs. 4(c) and (d), $D_{e\text{ ano}}$ decreases and $V_{e\text{ ano}}$ get to zero with increasing electron density, consistent with decreasing turbulence. In the high-density regime, $D_{e\text{ ano}}$ decreases with increasing electron density in the H plasma and increases in the D plasma. Importantly, $D_{e\text{ ano}}$ is suppressed in the D plasmas, which is qualitatively consistent with the suppression of turbulence. The outward convection velocity in the D plasma is qualitatively consistent with the electron density profile with a strong hollow in the D plasma; however it is inconsistent with the electron density dependence of the electron density fluctuations as well as with the suppression of the fluctuations in the D plasma. This is because the modulation amplitude is localized in the periphery in the high-density plasma, and the particle transport coefficient evaluated by the modulation becomes different from the equilibrium one owing to the spatial variation of the modulation amplitude.

6. TURBULENCE IDENTIFICATION

The previous sections suggest that the appearance of confinement and transport isotope effects in LHD is due to the isotope effect of turbulence. Furthermore, the measured turbulence has a different in the electron density dependence and isotope effects in the density regime, implying that the dominant turbulence mode differs depending on the density regime. Therefore, the identification of turbulence mode is essential in order to reveal the isotope effect of the plasma confinement in LHD. To investigate the dominant turbulence mode, the GyroKinetic Vlasov (GKV) simulation code [29, 30] carried out linear

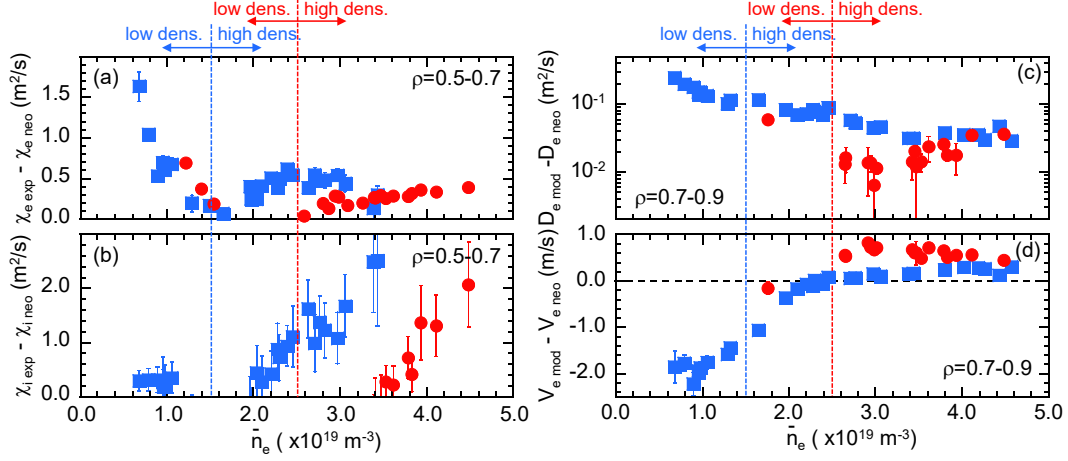


FIG. 4. Electron-density dependence of anomalous contribution of (a) electron energy transport, (b) ion energy transport, (c) diffusion coefficient and (d) convection velocity. The energy transport is averaged at $\rho=0.5-0.7$, and the particle transport is averaged at $\rho=0.7-0.9$

gyrokinetic calculations of the local flux tube for $k_{\rho i}=0.05-1.0$ which corresponds to the measurement region of 2D-PCI, including the effects of non-adiabatic electrons, collisionality and electromagnetic. The species included were electrons and bulk ions (H or D).

Figure 5(a) shows the density dependence of the linear growth rate calculated by GKV. The calculations were carried out for $\rho=0.5-0.7$, and the maximum values of γ_{ITG} are plotted. All calculations indicate that the real frequency is in the i-dia direction and its linear growth rate is that of the ITG turbulence γ_{ITG} . The linear growth rate decreases with increasing electron density due to the stabilizing effect of collisions, one of the characteristics of ITG turbulence. In the low-density regime, the density dependence and propagation direction of the linear-growth rate agree qualitatively with the experimental observation, suggesting the measured turbulence is ITG turbulence. However, the turbulence observed in the high-density regime is inconsistent with the characteristics of the ITG turbulence in terms of the electron density dependence, isotope effects, and propagation direction, suggesting that the appearance of other turbulences that cannot be treated by the GKV. An alternative candidate for turbulence is the resistive interchange (RI) turbulence, one of the interchange-type instabilities with a zero wavenumber in the direction of the magnetic field lines, which cannot be treated by GKV. The RI instability is the most unstable MHD instability, because an averaged magnetic curvature is bad in LHD, and it has been reported that not only the macroscopic low n/m modes but also the turbulent modes exist and play a role in confinement [31]. However, present GKV cannot handle RI turbulence, thus, we employed two-fluid MHD simulations to estimate the linear growth rate of RI turbulence γ_{RI} . We carried out the simulation at $\rho = 0.55$, where a clear turbulence peak exists. As shown in Fig. 5(b), γ_{RI} is stable in the low-density regime, but unstable at the high-density regime in both the H and D plasmas. Moreover, the lower γ_{RI} in D plasma at the high-density regime are qualitatively consistent with the lower turbulence level in D plasma. The low γ_{RI} values in D plasma are due to the lower resistivity, the lower pressure gradient due to the hollow density profile, and the heavier ion mass ($\gamma_{RI} \propto m^{-1/3}$) [32].

7. SUMMARY

In this paper, the behavior of ion-scale electron density fluctuations in electron density scan experiments under constant heating conditions was discussed in detail to understand the confinement improvement observed in LHD ECRH deuterium plasmas reported in a previous study [8]. We deduced that the LHD ECRH plasma can be divided into two confinement regimes depending on the dominant turbulence mode, which plays an important role in the appearance of isotope effects. The low-density regime is dominated by the ion-temperature gradient turbulence, with no isotope effects on the energy confinement time and transport as well as turbulence. The ITG turbulence is stabilized by collisions as the electron density increases, and at the same time, the resistive-interchange turbulence is excited because of the increased resistivity with the temperature increment. The low turbulence levels observed in D plasmas in the high-density regime are due to the suppression of RI turbulence by the low resistivity, low pressure gradient, and heavy ion masses, which contribute to improved confinement in D plasma. Therefore, the underlying mechanism of the isotope effect in ECRH plasma in LHD is due to the change in the dominant ion-scale turbulence from the ion temperature gradient turbulence to resistance exchange turbulence as the electron density increases.

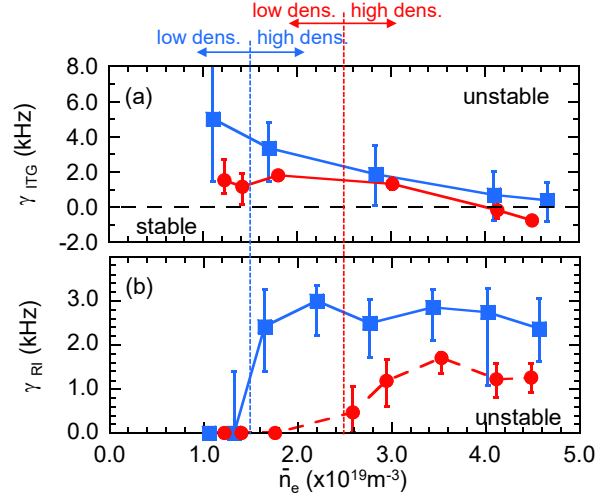


FIG. 5. Electron-density dependence of the linear growth rate of (a) ITG turbulence (γ_{ITG}) and (b) RI turbulence (γ_{RI}). We evaluated the error in γ_{ITG} and in γ_{RI} by changing the normalized ion-temperature gradient and pressure gradient by 20%, respectively.

ACKNOWLEDGEMENTS

LHD data can be accessed from LHD data repository at https://www-lhd.nifs.ac.jp/pub/index_e.html. The authors would like to thank all the members of the LHD Experiment group for their excellent work. The GKV simulations were performed on Plasma Simulator at NIFS. This work is supported by NIFS Grants (18ULHH013, 19ULHH013, 20ULHH013 and 21ULHH013) and JSPS Grants (21J12314, 16H04620 and 21H04458).

REFERENCES

REFERENCES

- [1] WEISEN, H. et al., *Journal of Plasma Physics* **86** (2020).
- [2] STROTH, U. et al., *Nuclear Fusion* **36** (1996) 1063.
- [3] STROTH, U., *Plasma physics and controlled fusion* **40** (1998) 9.
- [4] HIRSCH, M. et al., *Plasma Physics and Controlled Fusion* **50** (2008) 053001.
- [5] YAMADA, H. et al., *Nuclear Fusion* **45** (2005) 1684.
- [6] YAMADA, H. et al., *Physical Review Letters* **123** (2019) 185001.
- [7] TANAKA, K. et al., *Plasma Physics and Controlled Fusion* **62** (2019) 024006.
- [8] TANAKA, K. et al., *Nuclear Fusion* **59** (2019) 126040.
- [9] TANAKA, K. et al., *Plasma Physics and Controlled Fusion* **63** (2021) 094001.
- [10] BONANOMI, N. et al., *Nuclear Fusion* **59** (2019) 096030.
- [11] GARCIA, J. et al., *Nuclear Fusion* **57** (2016) 014007.
- [12] TANAKA, K. et al., *Review of Scientific Instruments* **79** (2008) 10E702.
- [13] MICHAEL, C. et al., *Review of Scientific Instruments* **86** (2015) 093503.
- [14] SHOJI, M. et al., *Journal of nuclear materials* **313** (2003) 614.
- [15] OISHI, T. et al., Effect of deuterium plasmas on carbon impurity transport in the edge stochastic magnetic field layer of large helical device, in *27th IAEA Fusion Energy Conference, Gandhinagar, India*, pages 22–27, 2018.
- [16] TSUJIMURA, T. I. et al., *Nuclear Fusion* **55** (2015) 123019.

- [17] YOKOYAMA, M. et al., Nuclear Fusion **57** (2017) 126016.
- [18] BEIDLER, C. et al., Plasma physics and controlled fusion **36** (1994) 317.
- [19] WEISEN, H. et al., Plasma physics and controlled fusion **30** (1988) 293.
- [20] CORDEY, J. et al., Nuclear Fusion **39** (1999) 1763.
- [21] URANO, H. et al., Physical Review Letters **109** (2012) 125001.
- [22] MAGGI, C. et al., Plasma Physics and Controlled Fusion **60** (2017) 014045.
- [23] WARMER, F. et al., Nuclear Fusion **58** (2018) 106025.
- [24] TANAKA, K. et al., Review of Scientific Instruments **87** (2016) 11E118.
- [25] GENTLE, K. et al., Plasma physics and controlled fusion **29** (1987) 1077.
- [26] OHTANI, Y. et al., Plasma Physics and Controlled Fusion **62** (2020) 025029.
- [27] TANAKA, K. et al., Nuclear fusion **46** (2005) 110.
- [28] TANAKA, K. et al., Fusion Science and Technology **58** (2010) 70.
- [29] WATANABE, T.-H. et al., Nuclear Fusion **46** (2005) 24.
- [30] NUNAMI, M. et al., Physics of Plasmas **27** (2020) 052501.
- [31] WATANABE, K. et al., Physics of Plasmas **18** (2011) 056119.
- [32] CARRERAS, B. et al., Physics of Fluids B: Plasma Physics **5** (1993) 1491.